Available online at www.sciencedirect.com
ScienceDirect
Journal of Magnetic Resonance 192 (2008) 101–111
JMR Journal of Magnetic Resonance
www.elsevier.com/locate/jmr

Spin state selective coherence transfer: A method for discrimination and complete analyses of the overlapped and unresolved ^{1}H NMR spectra of enantiomers

Bikash Baishya [a], Uday Ramesh Prabhu [a], N. Suryaprakash [b,*]

[a] *Solid State and Structural Chemistry Unit, Indian Institute of Science, Bangalore 560 012, India*
[b] *NMR Research Centre, SIF, Indian Institute of Science, Bangalore 560 012, India*

Received 28 November 2007; revised 11 January 2008
Available online 12 February 2008

Abstract

In general, the proton NMR spectra of chiral molecules aligned in the chiral liquid crystalline media are broad and featureless. The analyses of such intricate NMR spectra and their routine use for spectral discrimination of *R* and *S* optical enantiomers are hindered. A method is developed in the present study which involves spin state selective two dimensional correlation of higher quantum coherence to its single quantum coherence of a chemically isolated group of coupled protons. This enables the spin state selective detection of proton single quantum transitions based on the spin states of the passive nuclei. The technique provides the relative signs and magnitudes of the couplings by overcoming the problems of enantiomer discrimination, spectral complexity and poor resolution, permitting the complete analyses of the otherwise broad and featureless spectra. A non-selective 180° pulse in the middle of MQ dimension retains all the remote passive couplings. This accompanied by spin selective MQ–SQ conversion leads to spin state selective coherence transfer. The removal of field inhomogeneity contributes to dramatically enhanced resolution. The difference in the cumulative additive values of chemical shift anisotropies and the passive couplings, between the enantiomers, achieved by detecting *N*th quantum coherence of *N* magnetically equivalent spins provides enhanced separation of enantiomer peaks. The developed methodology has been demonstrated on four different chiral molecules with varied number of interacting spins, each having a chiral centre.

Keywords: Spin state selection; Triple quantum; Multiple quantum; Chiral discrimination; PBLG; Product operator; Spectral analyses

1. Introduction

The enatiomeric discrimination by NMR spectroscopy is a well established tool [1,2]. The derivation of this information from the isotropic media using chiral derivatising agents is not routinely feasible. On the other hand the weakly aligned chiral liquid crystalline media has been extensively employed as an alternate to isotropic media [3]. The degree of ordering in the chiral media is several orders of magnitude smaller than in achiral thermotropic nematic liquid crystalline phase. The orientational parameters of the two enantiomers are not identical and this fact has been exploited for their discrimination and also to determine enantiomeric excess (ee). The difference between the order parameters of the enantiomers is of the order of 10^{-3}–10^{-5} [4]. Nevertheless, it has a significant effect on the anisotropic NMR spectral parameters like chemical shift ($\Delta\sigma_i$) anisotropies, dipolar couplings (D_{ij}) and quadrupolar couplings (Q_i). As far as the proton detection is concerned, many a time the difference in $\Delta\sigma_i$ between the enantiomers is not significant and the transitions are indistinguishably overlapped. Hence $\Delta\sigma_i$ is not a suitable and exclusive parameter for visualizing enantiomers. However, the overlapped spectra with double the number of transitions are required to be unraveled before the analyses. Therefore, the dipolar couplings among protons, being more sensitive

* Corresponding author. Fax: +91 80 2360 1550.
E-mail address: nsp@sif.iisc.ernet.in (N. Suryaprakash).

1090-7807/$ - see front matter © 2008 Elsevier Inc. All rights reserved.
doi:10.1016/j.jmr.2008.02.005

to order parameters, are the obvious choice for such a purpose. Even though the spins are dipolar coupled, unlike in thermotropic liquid crystals, the spin systems are weakly coupled. Thus the spectra are amenable to first order analyses analogous to that of liquid state spectra. But the biggest bottleneck is the unresolved transitions from several short and long distance dipolar couplings. Furthermore, when the number of interacting spins increases, there is an excessive broadening preventing the analyses, which precludes the unraveling of the transitions for each enantiomer. Several methods to visualize the enantiomers using ^{1}H, ^{13}C, ^{19}F and extensive ^{2}H detection are available in the literature [5–19]. Each of these techniques has several distinct advantages and aids in chiral discrimination. Proton detection on the other hand is always advantageous because of high sensitivity due to high magnetic moment, high natural abundance, abundant presence in all the chiral organic molecules and enormous saving in experimental time. However, in the literature, the analyses of proton spectra have been described as difficult in complicated systems. Therefore, the development of any experimental methodology for enhancing the spectral resolution and simplification finds potential application.

The spin state selective detection is an important experimental tool that can be employed for such a purpose. In the spin state selective detection the high field and low field components of the multiplet are separated. This is an invaluable method for measuring very small couplings in biological macromolecules and also in high resolution solid state NMR studies. Several variants of this method to derive spectral information are reported in the literature [20–38].

Our recent work on selective detection of single quantum (SQ) transitions based on the spin states of the hetero nuclei [39] removed the redundancy of the SQ transitions required for extracting the coupling information. We have extended this MQ (multiple quantum) technique for the study of weakly aligned chiral molecules in the chiral liquid crystal media and developed the DQ-SERF (Double Quantum Selective Refocusing) experiment which does not utilize the spin state selection but provided unraveling of the overlapped peaks of the selectively excited methyl proton resonances [40]. In DQ-SERF excitation of double quantum coherence of methyl protons and retention of passive couplings among methyl protons results in higher resolution in double quantum dimension. However, single quantum dimension displays all the transitions arising from all the couplings and still remains complex. Further we have developed a methodology which is a blend of multiple quantum excitation and spin state selection. The spin state selection is achieved by spin selective correlation of higher quantum coherence to single quantum coherence of isolated coupled spins and retention of all the passive couplings in both the dimensions. This results in higher resolution in higher quantum dimension in spite of retention of all the couplings. Furthermore, the spin state detected fewer number of transitions provides even higher resolution in the SQ dimension. On the contrary, in DQ-SERF because of the refocusing of the remote passive couplings in DQ dimension, spin state selective detection could not be achieved and the spectra in the direct dimension is still complex. Thus the present work is superior as it simplifies the complex multiplet pattern, provides dramatically enhanced resolution both in SQ and MQ dimensions, separates the active (short distance) and passive (long distance) couplings for each enantiomer and achieves enantiomeric discrimination. The complete spectral information could be extracted, which was impossible from the unresolved one dimensional ^{1}H spectrum. The detailed understanding of the work is discussed. The elegant technique is robust and the pulse sequence is easy to implement.

2. Experimental confirmation

For the demonstration of the new experimental methodology, the molecules (*R*/*S*)-2-chloropropanoic acid (**1**), (*R*/*S*)-3-butyn-2-ol (**2**), (*R*/*S*)-propylene carbonate (**3**) and (*R*/*S*)-propylene oxide (**4**), each having a chiral centre were chosen. The samples were purchased from Sigma. The racemic structures of these molecules are given in Fig. 1. The oriented samples were prepared by the method described in the literature [10,15]. For the oriented sample **1**, 50 mg of the racemic sample, 80 mg of poly-γ-benzyl-L-glutamate (PBLG) and 300 mg of $CDCl_3$ were taken. For aligned sample **2**, 85 mg of PBLG, 59 mg of (*R*/*S*)-3-butyn-2-ol procured from Sigma and 450 mg of $CDCl_3$ were taken. For aligned sample **3**, 54 mg of **3**, 102.8 mg of PBLG and 665 mg of $CDCl_3$ were taken. For oriented sample **4**, 42.5 mg of the sample, 78 mg of PBLG with DP 782 procured from Sigma and 580 mg of $CDCl_3$ were taken. The samples were sealed in a 5 mm NMR tube to avoid the evaporation of the solvent and then centrifuged back and forth for several hours till the visually homogeneous phase was observed. The orientation of the sample

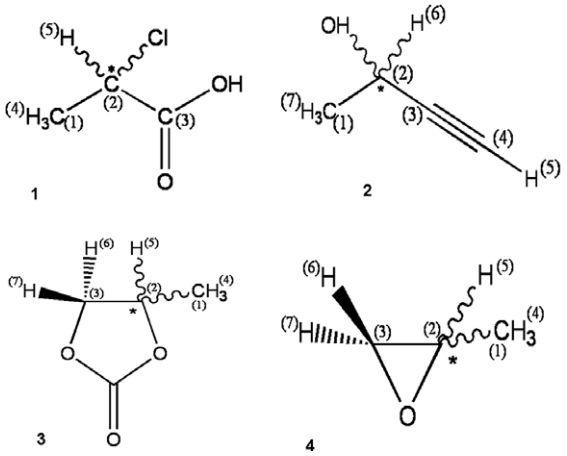

Fig. 1. The racemic structures and number of interacting spins in (**1**) (*R*/*S*)-2-chloropropanoic acid, (**2**) (*R*/*S*)-3-butyn-2-ol, (**3**) (*R*/*S*)-propylene carbonate and (**4**) (*R*/*S*)-propylene oxide.

was investigated by monitoring the ^{2}H doublet separation of $CDCl_3$. The temperature was maintained at 300, 300.7, 300 and 303 K for **1**, **2**, **3**, **4**, respectively, using Bruker BVT 3000 temperature controller unit of the DRX-500 NMR spectrometer. The one dimensional proton spectra of all the molecules with expanded regions and assignments to different protons taken from the literature [4, 7, 10 and 11] are given in Fig. 2. The spectral complexity progressively increases on going from top trace to bottom trace. The real challenge is the analyses of the spectra of **3** and **4**, which are broad and featureless.

The spin selective excitation of the triple quantum (3Q) coherence of coupled spins is the basis of this new methodology. The pulse sequence utilized for this experiment is given in Fig. 3a [41]. In the indirect dimension (t_1 dimension) the MQ coherence is allowed to evolve and at the end of the t_1 period, the magnetization is converted back to single quantum coherence for detection (t_2 dimension).

To excite 3Q quantum coherence in an A_3 spin system like methyl protons, the delay, τ, between the first and the second 90° pulses should be $1/2(^2T_{HH})$, where $^2T_{HH}$ (which corresponds to $3(^2D_{HH})$) refers to the separation between the adjacent transitions of the triplet arising from the coupling of protons that are two bonds away. The 3Q excitation is maximum for 1/2 ($3 \times {}^2D_{HH}$). This can be understood using the product operator formalism [42]. For an A_3 spin system, the spin operator terms present just before the second 90° pulse of the pulse sequence shown in Fig. 3a at the position A are;

$$-I_Y \cos^2 \pi(^2T_{HH})\tau + 2I_X S_Z \sin 2\pi(^2T_{HH})\tau + 2I_Y S_Z R_Z \times \sin^2 \pi(^2T_{HH})\tau \quad (1)$$

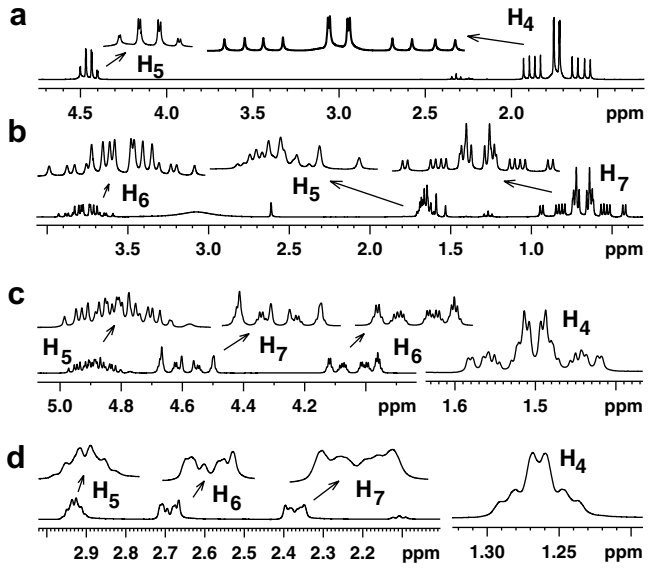

Fig. 2. From top to bottom: 500 MHz one dimensional ^{1}H spectrum of (*R*/*S*)-2-chloropropanoic acid; (*R*/*S*)-3-butyn-2-ol, (*R*/*S*)-propylene carbonate and (*R*/*S*)-propylene oxide respectively. The expansions of the particular regions of each spectrum and the assignment to different protons are shown.

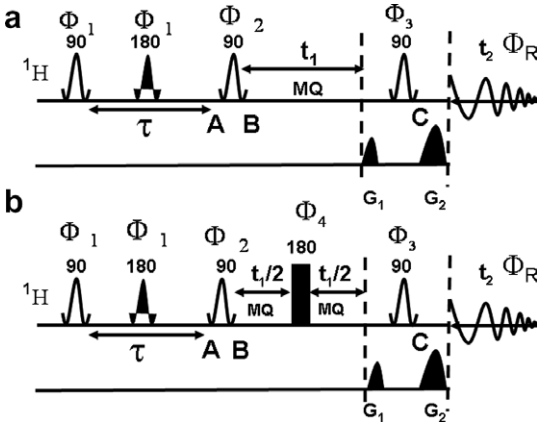

Fig. 3. (a) The pulse sequence used for the selective excitation of 3Q coherence of methyl group for the molecules **1** and **2**. The phases of the pulses are; $\Phi_1 = (12)$ X, $\Phi_2 = (12)$ Y, $\Phi_3 =$ Y and $\Phi_R =$ X and the selection of the higher quantum coherence is by the gradients; (b) The pulse sequence used for the selective excitation of 3Q coherence of methyl group for the molecules **3** and **4**. The phases of the pulses are; $\Phi_1 = (12)$ X, $\Phi_2 = (12)$ Y, $\Phi_3 =$ Y, $\Phi_4 =$ X and $\Phi_R =$ X. Triple Quantum EXORCYCLE phase cycling is used for the non-selective 180° pulse (to remove field inhomogeneity) in the middle of 3Q dimension. The phase cycling of odd and even quantum schemes are different [43].

where the term $I_Y S_Z R_Z \sin^2\pi(^2T_{HH})\tau$ is converted into a 3Q coherence by the 2nd 90° pulse of phase *y*. The experimentally found optimum values of τ generally do not agree with the theoretical one. This is because the MQ excitation is non uniform [43]. A detailed discussion of the optimization of τ delay and its effect on the intensity of the peaks and the problems and prospects of enantiomeric excess measurement has already been reported [40].

Three types of MQ experiments have been carried out, viz., (a) selective excitation of isolated methyl proton resonances of all the molecules, (b) bi-selective excitation of methine and acetylenic protons in **2** and (c) selective excitation of methine and methylene protons in **3** and **4**.

In **1**, the methyl and methine resonances are well separated. The spectrum is a overlap of transitions from *R* and *S* enantiomers with the 140 Hz bandwidth for the methyl region. Thus it was possible for the simultaneous and selective excitation of the methyl protons of both the enantiomers. However, the challenge was the differential dipolar couplings among the protons of the methyl group in each enantiomer. As discussed in the earlier work [40], a series of two dimensional experiments were carried out to optimize the τ delay for maximizing the signal intensity for the methyl group. The intensity of the spectrum for the first t_1 incremental delay corresponding to each enantiomer was monitored as a function of τ delay. The average delay which gave maximum and comparable signal intensities for both the enantiomers was chosen. Identical procedure was followed for all the other molecules and the acquisition and processing parameters are reported in the corresponding figure captions. All the spectra are reported in magnitude mode.

3. Theory of spin state selective MQ–SQ correlation

The detailed theoretical description is available as additional material. However, the few salient and relevant points are discussed below. As the spectra in PBLG medium is first order, for the theoretical understanding of the present spin state selective correlation is discussed in our earlier work [44]. The only difference between isotropic case and PBLG studies is that J_{ij} is replaced by T_{ij} where $T_{ij} = J + 2D_{ij}$ for nonequivalent spins and $T_{ij} = 3D_{ij}$ for equivalent spins.

For spin state selective coherence transfer, two points are of vital importance; (a) couplings to a passive spin should be retained in both the MQ and SQ dimensions and (b) the MQ–SQ conversion is carried out with spin selective pulse without disturbing the states of the passive spin. In such an experiment the $|\alpha>$ domain MQ coherence is correlated to $|\alpha>$ domain SQ coherences only and there is no coherence transfer to the $|\beta>$ domain SQ coherences. The same analogy holds good for $|\beta>$ domain MQ coherence. This is an important difference when compared to conventional MQ–SQ correlation experiment where MQ–SQ conversion is carried out with non-selective pulses.

Some important features of this methodology in the context of enantiomeric discrimination required to be highlighted are; (i) A complex multiplet that is difficult to analyze in one dimensional proton spectrum can be separated into individual sub spectra in different cross sections depending on the passive spin states thereby achieving spectral simplification. This separates the active and passive couplings and achieves very high resolution in both MQ and SQ dimensions, (ii) active couplings are present in each SQ cross section corresponding to each passive spin state in MQ dimension, (iii) the displacements between different sub spectra provide the passive couplings and (iv) the relative signs of the couplings can be determined from the comparison of the tilts of the displacement vector unlike any of the earlier reported experiments including DQ-SERF.

DQ-SERF is also a spin selective MQ–SQ correlation experiment. Nevertheless, significant difference arises from the fact that in DQ-SERF the methyl proton spin selective refocusing pulse is utilized in the middle of the DQ dimension to achieve high resolution by removing the existence of remote passive couplings. As an example in (*R*/*S*)-propylene oxide the coupling of methyl protons to methylene protons and the methine proton are removed. However, for spin state selective coherence transfer like in the present study the existence of the remote couplings in the MQ dimension is crucial.

4. Results and discussion

4.1. (*R*/*S*)-2-chloropropanoic acid

The signal from the hydroxyl proton is broadened and it does not display coupling to other protons. Thus the spin system of the protons in **1** is of the type A_3X where A refers to methyl protons and X corresponds to methine proton. The one dimensional ^{1}H spectrum in the chiral liquid crystal PBLG shown in Fig. 2a has well separated peaks for methyl and methine protons. The methyl protons are split into 1:2:1 triplet due to residual proton dipolar couplings among magnetically equivalent protons. The separation between two adjacent transitions provides $^2T_{HH}$ ($=3x^2D_{HH}$), where T refers to the sum of dipolar couplings and the superscript 2 refers to the proton that is two bonds away. Due to magnetic equivalence, J_{HH} does not influence the spectrum and the separation of two consecutive transitions directly provides ($3 \times {}^2D_{HH}$). Each of these transitions is further split into doublets of equal intensity due to coupling with methine proton. Thus the six transitions observed can be visualized as two A_3 sub spectra corresponding to two passive spin states of X spin. One of the A_3 sub spectra corresponds to methine proton in the $|\alpha>$ state and the other for the methine proton in the $|\beta>$ state. The methine proton is a quartet due to its coupling with methyl protons.

2D spectrum correlating the 3Q–SQ coherence of methyl group is shown in Fig. 4 along with the corresponding projections. The assignments to *R* and *S* enantiomers are taken

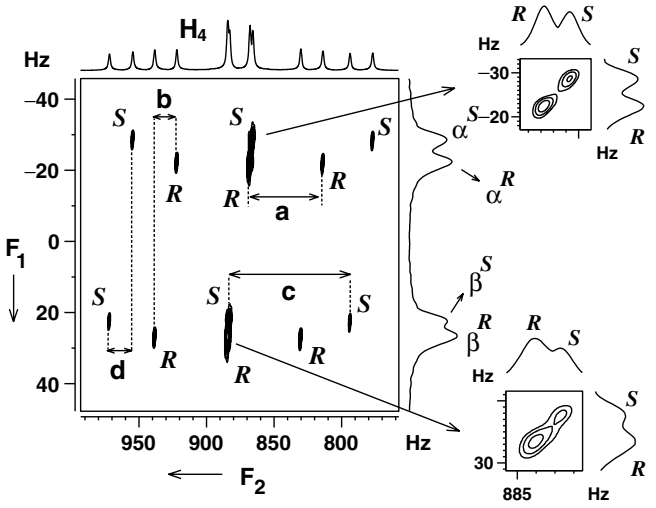

Fig. 4. 2D 3Q–SQ spectrum of (*R*/*S*)-2-chloropropanoic acid of methyl protons along with F_1 and F_2 projections. The t_1 and t_2 dimensions corresponds to 3Q and SQ dimensions. The 2D data matrix is 1331 × 416 and zero filled to 4 and 2 k points before processing. The sine bell window function is used in both the dimensions. Four scans for each FID and a recycle delay of 4 s. The optimized τ delay is 41 ms. The seduce shaped pulse lengths are 1.38 ms at 36 db for 90° and the length is 2.76 ms for 180° pulses. Digital resolution is 0.14 and 0.07 Hz in F_1 and F_2 dimensions. Assignment for the enantiomers *R* and *S* is taken from the literature [9]. $|\alpha_R>$, $|\beta_R>$ and $|\alpha_S>$, $|\beta_S>$ are the two spin states of the passive spin for the enantiomers *R* and *S*, respectively. The separations (in Hz) depicted in alphabets provide coupling information. For *R* enantiomer: $a = {}^2T_{H4H4} = 54.1$ Hz and $b = {}^3T_{H4H5} = 16.4$ Hz. For *S* enantiomer; $c = {}^2T_{H4H4} = 88.8$ Hz, $d = {}^3T_{H4H5} = 17.3$ Hz. The expansion of the two regions of the spectrum shown clearly identifies the two peaks of the enantiomers. Notice the advantage of spin state selection and scaling of the coupling to resolve the peaks shown in two expanded regions.

from the literature [9]. The separation of the two A_3 sub spectra from each other, for each enantiomer, into different cross sections is clearly evident. The spin selected 3Q coherence of the methyl protons evolves at the sum of the resonance offsets of all the A spins (chemical shifts can be treated as zero due to magnetic equivalence of all the three protons) under the sum of the passive couplings $^3T_{HH}$. In the 3Q dimension A_3X spin system behaves like an AX spin system, where A is the super spin and the 3Q spectrum corresponds to A part of the AX spectrum and display a doublet. This doublet separation is $3(^3T_{HH}) = 3(2D_{HH} + J_{HH})$ rather than $^3T_{HH}$ between adjacent SQ transitions in a SQ spectrum and plays a prominent role in enhanced separation of enantiomer peaks. The basic symmetry functions for an A_3 spin systems is already reported in our earlier work [40]. There are two 3Q transitions for each enantiomer which are, $|\alpha_A\alpha_A\alpha_A(\alpha_X)> \rightarrow |\beta_A\beta_A\ \beta_A(\alpha_X)>$ and $|\alpha_A\alpha_A\alpha_A\ (\beta_X)> \rightarrow |\beta_A\beta_A\beta_A(\beta_X)>$, corresponding to $|\alpha>$ and $|\beta>$ spin states of passive spin X.

The one dimensional proton spectrum corresponding to the methyl region and the cross sections taken on the SQ dimension at different spin states of 3Q dimension of Fig. 4 is plotted in Fig. 5a–f. Each of these cross sections is a triplet and pertains to sub spectrum according to $|\alpha>$ and $|\beta>$ spin states of the passive proton. Thus the spin state selective detection of A_3 SQ transitions is achieved. For the transition within each sub spectrum, the spin state of X remains the same in both t_1 and t_2 dimensions. Thus the coupling to remote proton is removed in each cross section resulting in half the number of transitions compared to one dimensional spectrum and hence high resolution in SQ dimension. This allows the precise measurement of $^2T_{HH}$. Therefore, in a single experiment not only one can determine both $^2T_{HH}$ and $^3T_{HH}$ but also separate them which was not possible from any earlier reported experiments including DQ-SERF. This reduces the spectral complexity arising out of too many couplings leading to unresolved transitions in a single dimension (one dimensional ^{1}H spectrum) and aids in the simplification of enantiomer spectra. In an earlier study using the nonselective MQT experiment [8] in a strongly orienting media, there is no spin state selection and all the short and long distance couplings in the molecule are present in each cross section and hence no spectral simplification.

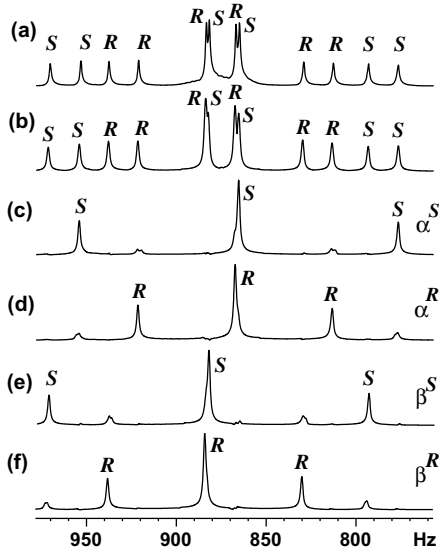

Fig. 5. (a) The methyl region of the one dimensional ^{1}H spectrum of Fig. 1a and b) the projection of the 2D spectrum of Fig. 4. taken along the F_2 dimension and (c–f) the cross sections taken along F_2 for each spin state in the 3Q dimension of Fig. 4. α_S, α_R and, β_S, β_R are the two spin states for R and S enantiomers in the 3Q dimension.

In addition to dipolar couplings, there is also advantage due to the scaling of the chemical shift anisotropy for chiral discrimination. The difference in anisotropic chemical shifts between the R and S enantiomers in the SQ dimension is 4.6 Hz. Though it is possible to visualize in the one dimensional spectra (Fig. 2a), it is better visualized in 3Q dimension (Fig. 4). Due to magnetic equivalence of methyl protons, this value is also enhanced three times, i.e., 13.8 Hz in the 3Q dimension which can be viewed after discrimination by comparing the centre of the two separated spectra.

All the separations which provide spectral parameters, viz., $a = {}^2T_{H4H4}$, $b = {}^3T_{H4H5}$ for the R enantiomer and $c = {}^2T_{H4H4}$, $d = {}^3T_{H4H5}$ for the S enantiomer are marked in Fig. 4. These values are reported in the figure caption.

4.2. (R/S)-3-butyn-2-ol

The protons of **2** form a spin system of the type A_3MX. The one dimensional ^{1}H spectrum given in Fig. 2b has well resolved peaks for the CH_3 and two CH groups. The peak due to hydroxyl proton is broadened and do not display coupling pattern from any other protons. The methyl protons experience three different type of couplings, viz. (a) coupling among themselves ($^2T_{HH}$) leading to a triplet, (b) coupling between methyl and methine (M-spin) proton ($^3T_{HH}$) giving a doublet for each transition of the triplet, (c) coupling between methyl and acetylenic (X-spin) proton ($^5T_{HH}$) giving a doublet of a triplet. The twelve transitions observed can be construed as four A_3 sub spectra corresponding to four possible passive spin states of M and X spins together.

In the 3Q dimension the spin system is of the type AMX, where A is a super spin with three methyl protons, M and X are the protons from the methine and acetylenic groups, respectively. The 3Q dimension is the A part of the AMX spin system where the magnetization evolve under the sum of the passive couplings. The 2D 3Q–SQ spectrum and the assignments of peaks to R and S taken from the literature [4], along with the F_1 and F_2 projections are given in Fig. 6. Our spectral parameters are substantially different from the literature values. However, we have adopted the trend that the larger coupling is from R enantiomer in making assingments. Corresponding to four spin states $|\alpha\alpha>$, $|\alpha\beta>$, $|\beta\alpha>$ and $|\beta\beta>$ of the passive spins M and X, there are four allowed 3Q transitions for A spin arising

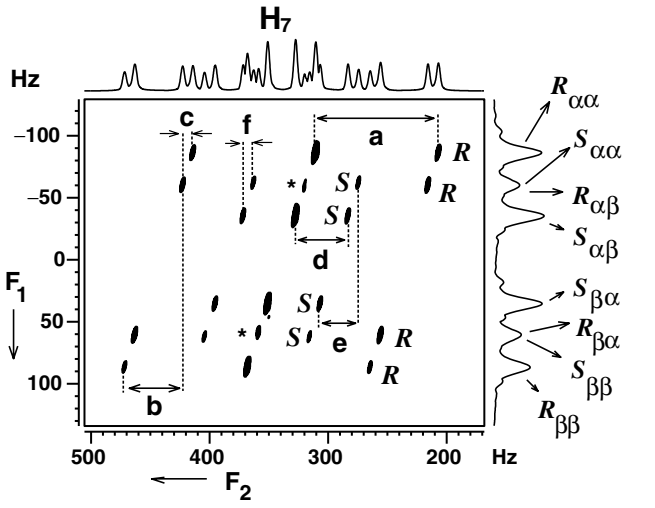

Fig. 6. 2D 3Q–SQ spectrum of (*R*/*S*)-3-butyn-2-ol with F_1 and F_2 projections. The 2D data matrix is 1228 × 336 and zero filled to 4 and 1 k before processing. The sine bell window function is used in both the dimensions. Four scans for each FID and a recycle delay of 7 s. The optimized τ delay is 10 ms. The seduce shaped pulse lengths are 6.25 ms for both 90° and 180° pulses with different power levels. Digital resolution is 0.5 and 0.1 Hz in F_1 and F_2 dimensions. The assignments of the enantiomers *R* and *S* are taken from the literature [4]. The $R_{\alpha\alpha}$, $R_{\alpha\beta}$, $R_{\beta\alpha}$ and $R_{\beta\beta}$ and $S_{\alpha\alpha}$, $S_{\alpha\beta}$, $S_{\beta\alpha}$ and $S_{\beta\beta}$ are used to indicate spin states of the passive protons for the enantiomers *R* and *S*, respectively. The separations (in Hz) depicted in alphabets provide coupling information. For *R* enantiomer: $a = {}^2T_{H7H7} = 103.4$ Hz, $b = 3({}^3T_{H6H7}) = 48.9$ Hz and $c = 3({}^5T_{H5H7}) = 8.8$ Hz. For *S* enantiomer; $d = {}^2T_{H7H7} = 44.3$ Hz, $e = 3({}^3T_{H6H7}) = 32.4$ Hz and $f = 3({}^5T_{H5H7}) = 9.0$ Hz. Note the quality of enantiomer discrimination achieved in the 3Q dimension.

from each enantiomer unlike 12 crowded transitions in a SQ spectrum. Thus spectrum in 3Q dimension gets highly resolved which aids in enantiomeric discrimination. From the previously published work [4] the spectrum with a higher degree of ordering was assigned to *R* enantiomer. The cross sections taken along the SQ dimension for each spin state of an enantiomer provides only the active coupling between the methyl protons, which is a triplet. There are four such triplets pertaining to four A_3 sub spectra in different cross sections. Thus high resolution is achieved also in SQ dimension. Four such cross sections with identical active coupling unambiguously differentiate the peaks arising from each enantiomer.

From the 3Q dimension the passive coupling information, ${}^3T_{HH}$ and ${}^5T_{HH}$, could be determined directly. The separation between the states $R_{\alpha\alpha}$ and $R_{\beta\alpha}$ or $R_{\alpha\beta}$ and $R_{\beta\beta}$ shown in Fig. 6 provides $3({}^3T^R_{HH})$, which is the sum of the scalar and dipolar couplings between the methyl protons and methine proton. Similarly, the separation between the states $S_{\alpha\alpha}$ and $S_{\beta\alpha}$ or $S_{\alpha\beta}$ and $S_{\beta\beta}$ provides $3({}^3T^S_{HH})$ for *S* enantiomer. The long distance coupling $3({}^5T_{HH})^{(R/S)}$, could also be obtained from the separations of the peaks corresponding to the spin states $R_{\alpha\alpha}$ and $R_{\alpha\beta}$ or $R_{\beta\alpha}$ and $R_{\beta\beta}$ for the *R* enantiomer and $S_{\alpha\alpha}$ and $S_{\alpha\beta}$ or $S_{\beta\alpha}$ and $S_{\beta\beta}$ for the *S* enantiomer. The derivable parameters from the respective displacements of the sub spectra $a = ({}^2T_{H7H7})$, $b = 3({}^3T_{H6H7})$, $c = ({}^5T_{H5H7})$, for *R* enantiomer and $d = ({}^2T_{H7H7})$, $e = ({}^3T_{H6H7})$ and $f = ({}^5T_{H5H7})$ for *S* enantiomer are marked in Fig. 6. The derived parameters are reported in the figure caption.

The dipolar coupling between methine and acetylenic protons, a parameter lacking for complete analysis, does not evolve either in the SQ dimension or in the 3Q dimension. This can be determined by a spin selective DQ–SQ spectrum of the methine and acetylenic protons. In this situation the DQ dimension pertains to A part of an AX_3 spin system giving rise to a quartet. The cross section taken along SQ dimension for each spin state in the DQ dimension provides a doublet due to active coupling between methine and acetylenic protons at their respective chemical shifts. This spectrum is not shown but the values for $({}^4T_{H5H6})^R$ and $({}^4T_{H5H6})^S$ are 21.1 and 13.6 Hz, respectively. The F_1 dimension provides a quartet for each enantiomer which gives the coupling to the methyl protons. This information is, however, redundant as it has already been obtained from the previous experiment. In an earlier study on this molecule [4], the enantiomers have been visualized using their excess and the iterative analyses have been carried out to derive all the spectral parameters. The information on the couplings determined from the present experiment can be used in such iterative analysis as the starting parameters. This also significantly simplifies the analysis of the one dimensional single quantum spectrum as the number of parameters required to be iterated are reduced.

4.3. (R/S)—propylene carbonate and (R/S)—propylene oxide

In **3** and **4**, protons form a weakly coupled spin system of the type A_3MNX where A_3 corresponds to active methyl protons, M and N are the two passive methylene protons and X is the methine proton. The methyl protons experience four different type of couplings, viz. (a) couplings among themselves $({}^2T_{HH})$ leading to a triplet, (b) coupling between methyl and methine (X-spin) proton $({}^3T_{HH})$ giving a doublet for each transition of the triplet, (c) coupling from the two diastereomeric methylene protons (M and N spins, protons numbered 6 and 7 in Fig. 1) $({}^4T_{HH})$ giving rise to further splitting of each transition to doublet of doublet. The twenty four transitions observed can be visualized as eight A_3 sub spectra corresponding to eight passive spin states of M, N and X together.

The one dimensional spectra of **3** and **4** are shown in Fig. 2c and d. The spectrum for the methyl region of both **3** and **4** consists of 48 transitions which is a mixture of spectra from the two enantiomers resonating within 90 Hz spectral width for **3** and 40 Hz for **4**. The broad and featureless spectrum due to small strengths of the long distance couplings makes it impossible to recognize any fine structure. Achieving both high resolution in 3Q dimension and spin state selective detection, in spite of very small couplings from the two methylene protons which is unresolved, is a big challenge. This is due to the contributions

of the field inhomogeneity at the higher quantum coherence. When the spatially dependent field inhomogeneity, $\Delta B_0(r)$, is taken into account, the precessional frequency of the higher quantum (ω_{HQ}) is given as

$$\omega_{HQ} = \sum \Delta m_I(\omega_I + \gamma_I \Delta B_0(sr)) \quad (2)$$

Thus the inhomogeneity contribution increases linearly with the detection of the higher quantum order. Therefore, the 3Q order has three times the enhanced signal broadening. One method to remove this field inhomogeneity contribution is to apply a non-selective 180° pulse in the middle of the t_1 dimension which refocuses the chemical shifts and retains all the passive couplings for spin state selection [43]. This pulse scheme (Fig. 3b), although improves the contour spread, was not essential for the two molecules discussed earlier as the transitions were sufficiently resolved.

The selective methyl protons excited two dimensional 3Q–SQ correlated spectrum of **3** is given in Fig. 7. In the 3Q dimension, the spin system is of the type AMNX. The three protons M, N and X are passive spins. $^2T_{HH}$ in A_3 are the active couplings while one $^3T_{HH}$ and two $^4T_{HH}$ constitute the passive couplings. The 3Q dimension provides eight transitions for each enantiomer pertaining to eight spin states of M, N and X. Assignments for *R* and *S* is taken from the literature [6]. For the *S* enantiomer the two types of $^4T_{HH}$ are equal and hence results in a triplet of a doublet (due to $^3T_{HH}$) in the 3Q dimension and are marked *S* in Fig. 7. However, for the *R* enantiomer the two types of $^4T_{HH}$ are unequal. Hence 3Q dimension provide eight distinct transitions marked *R* in the figure. Unlike the 48 transitions of one dimensional spectrum the 3Q spectrum contains only eight transitions which dramatically enhanced the resolution and visualization of enantiomers.

The cross sections taken along the SQ dimension for each passive spin state in 3Q dimension is a triplet due to active coupling $^2T_{HH}$. The eight A_3 sub spectra (triplets) for eight passive spin states are observed for *R* enantiomer. However, for *S* enantiomer, six triplets with smaller dipolar couplings are observed. The separations providing spectral parameters are; $a = {}^2T_{H4H4}$, $b = {}^3T_{H4H5}$, $c = d = {}^4T_{H4H6} = {}^4T_{H4H7}$ for the *S* enantiomer and $e = {}^2T_{H4H4}$, $f = {}^3T_{H4H5}$, $g = {}^4T_{H4H6}$, $h = {}^4T_{H4H7}$ for the *R* enantiomer are marked in Fig. 7. The coupling information among protons numbered, 5, 6 and 7 are not reflected either in the 3Q or in the SQ dimension.

For the determination of the complete spectral information another 3Q–SQ experiment with 5, 6 and 7 protons as active spins was carried out. This spectrum is shown in Fig. 8. In the 3Q dimension the spin system is of the type AX_3 where super spin A pertains to M, N and X spins and the methyl protons are the passive spins. The A part of this AX_3 is detected in the 3Q dimension. 3Q dimension is therefore a quartet for each enantiomer, indicated by tilted broken lines for four *R* and *S* transitions each. Active coupling $^2T_{H6H7}$ appearing at chemical shift positions of

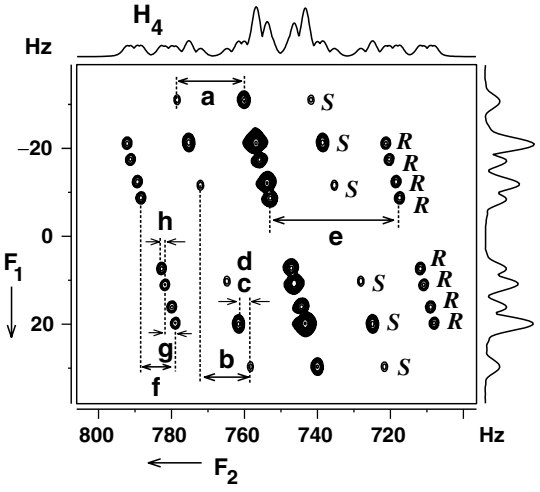

Fig. 7. Two dimensional 3Q–SQ spectra of selectively excited methyl protons in (*R*/*S*)-propylene carbonate. Assignments to *R* and *S* are taken from the literature [6]. The 2D data matrix is 368 × 96 and zero filled to 1 k and 256 points before Fourier transformation. The sine bell window function is used in both the dimensions. Eight scans for each FID and a recycle delay of 4 s. The optimized τ delay is 12.5 ms. The seduce shaped pulse lengths are 2.5 and 3 ms for 90° and 180° pulses, respectively. Digital resolution is 0.37 and 0.14 in F_1 and F_2 dimensions. The separations (in Hz) depicted in alphabets provide coupling information. For *S* enantiomer: $a = {}^2T_{H4H4} = 18.3$, $b = {}^3T_{H4H5} = 13.7$, $c = ({}^4T_{H4H6})$ and $d = {}^4T_{H4H7} = 3.2$. For *R* enantiomer; $e = {}^2T_{H4H4} = 35.4$, $f = {}^3T_{H4H5} = 9.5$, $g = ({}^4T_{H4H6}) = 2.8$ and $h = {}^4T_{H4H7} = 0.9$. Two types of $^4T_{HH}$ (between 4 and 6, between 4 and 7) are arbitrary for *R* enantiomer and they are equal for the *S* enantiomer.

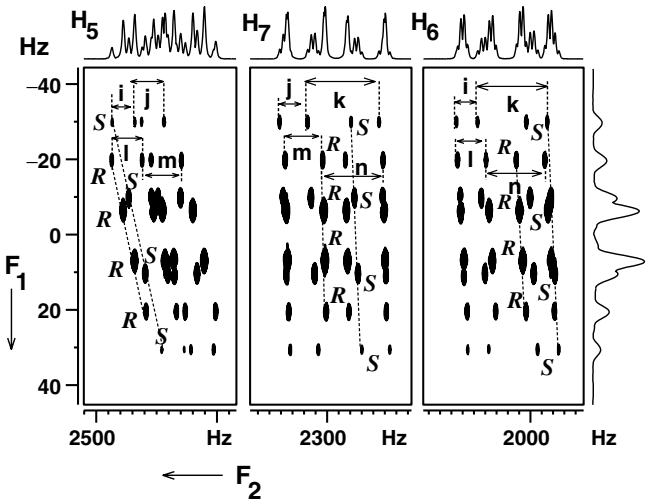

Fig. 8. Two dimensional 3Q–SQ correlation spectra of (*R*/*S*)-propylene carbonate with selective excitation of protons numbered 5, 6 and 7. The 2D data matrix is 1638 × 80 points and zero filled to 2 k and 256 points before Fourier transformation. The sine bell window function is used in both the dimensions. Eight scans for each FID and recycle delay is 4 s. The digital resolution is 0.35 and 0.31 in F_1 and F_2 dimensions. The optimized τ delay is 14.28 ms. The seduce shaped pulse length are 2.4 and 3.3 ms for the 90° and 180° pulses. The separations providing coupling information (in Hz) are marked. For *S* enantiomer; *i* ($^3T_{H5H6}$) = 18.4, *j* ($^3T_{H5H7}$) = 24.3, *k* ($^3T_{H6H7}$) = 61.8, For *R* enantiomer; *l* ($^3T_{H5H6}$) = 25.3, *m* ($^3T_{H5H7}$) = 32.7, *n* ($^3T_{H6H7}$) = 52.1.

both H6 and H7 is marked as k. At H7 position $^3T_{H5H7}$ (j) and at H6 position $^3T_{H6H5}$(i) are also marked. The right tilt of the quartet in each chemical shift position shown by broken line implies that all the passive couplings are of the same sign. The separations i, j and k for S enantiomer and l, m and n for R enantiomer are also marked in the figure. The passive couplings can also be determined from this experiment using the displacement vector. However, this information is redundant as it has already been obtained from the 3Q–SQ spectrum of methyl protons.

The one dimensional spectrum of **4** is more densely crowded than **3** as seen from the Fig. 2d. Therefore, the analyses of this spectrum is much more challenging than the previously discussed molecules. The 2D 3Q–SQ correlated spectrum of methyl group of **4** is reported in Fig. 9. The 3Q dimension provides eight well resolved transitions for S enantiomer. However, for the R enantiomer only four transitions are observed due to negligible strength of one of the remote couplings, which is clearly evident from the spectrum. This negligible strength of one of the remote couplings is possibly from the opposite signs of J_{HH} and D_{HH}. All the derivable parameters are marked in the figure and reported in the corresponding figure captions.

The 3Q–SQ spectrum involving protons numbered 5, 6 and 7 is shown in Fig. 10. The active couplings i, j and k for R enantiomer and l, m and n for the S enantiomer are marked in the figure. The H6 and H7 regions are better resolved than H5 region. Thus the quartet for S enantiomer is marked while only two lines of R enantiomer quartet are marked in the figure. Each cross section at H5, H6, H7 is a doublet of doublet because of two active couplings. Displacements marked e, f and g for R enantiomer and b, c and c^* for S enantiomer contains individual passive couplings of H5, H6 and H7 to methyl protons. This information is also obtainable from Fig. 9. This spectrum gives additional information on the relative signs of the couplings. The tilt direction at e is opposite to f and g indicating coupling e is opposite in sign to f and g. Similarly b has opposite sign to c. The separation between adjacent 3Q transitions marked P for S enantiomer is 5.3 Hz. Employing the relative signs of the couplings measured, it turns out to be 4.9 Hz ($\approx b + c + c^* = 6.3 - 1.4 - ?$, where c^* is immeasurably small and is within line width). Similarly for R enantiomer, the measured separation in the 3Q dimension is marked Q and is equal to 2 Hz. These values obtained by using the relative signs of the couplings is 1.95 Hz ($\approx e + f + g = 4.1 - 0.65 - 1.5$). This confirms the relative signs of the couplings determined.

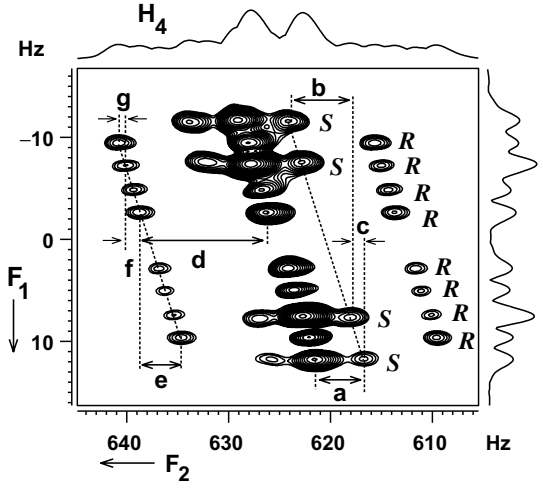

Fig. 9. Two dimensional 3Q–SQ spectra of selectively excited methyl protons in (R/S)-propylene oxide. The 2D data matrix is 224 × 128 and zero filled to 1 k and 512 points before processing. The sine bell window function is used in both the dimensions. Four scans for each FID and a recycle delay of 16 s. The optimized τ delay is 41.6 ms. The seduced shaped pulse lengths are 5 ms for both 90° and 180° pulses with different power levels. The digital resolution is 0.13 and 0.06 Hz in F_1 and F_2 dimensions, respectively. The separations (in Hz) represented by different alphabets provide coupling information. Assignments to R and S enantiomers are taken from the literature [10]. For S enantiomer: $a = {}^2T_{H4H4} = 4.7$, $b = {}^3T_{H4H5} = 6.3$ and $c = {}^4T_{H4H6} = 1.4$. The separation $^4T_{H4H7}$ is not detectable due to small strength. For R enantiomer: $d = {}^2T_{H4H4} = 12.5$, $e = {}^3T_{H4H5} = 4.1$, $f = {}^4T_{H4H6} = 1.5$ and $g = {}^4T_{H4H7} = 0.7$.

The advantages of the present study are several fold.

(a) The dramatic resolution has been achieved in the otherwise broad and featureless spectra and the peak separation of the order of 0.7 Hz could be measured.
(b) In both selective 3Q–SQ experiments, the values of $^nT_{HH}$ ($n = 2, 3, 4, 5$) being different for both the enantiomers, there was an unambiguous chiral discrimination in both the dimensions.
(c) Short and long distance couplings are separated from each other in a single experiment and both are utilized for discrimination.
(d) Using two 3Q–SQ experiments the complete analyses of the overlapped spectra of both enantiomers in **3** and **4** have been carried out.
(e) In the methyl group excited experiments the scaling of $^nT_{HH}$ by a factor of three in the 3Q dimension and one in the SQ dimension results in a net total chiral dispersion of 3.3 times as far as the measurement of the resonance frequencies between the chiral molecules are concerned in the tilted direction. The difference between consecutive R and S peaks $\{T^R (=^nT_{HH})\text{-}T^S (=^nT_{HH})\}$ becomes $3 \times \{T^R (=^nT_{HH})\text{-}T^S (=^nT_{HH})\}$ in 3Q dimension which contributed to better chiral discrimination. In the earlier SERF experiments the consecutive R and S peak separation was only $\{T^R (=^nT_{HH})\text{-}T^S (=^nT_{HH})\}$ [5].
(f) The difference in CSA between the two enantiomers is also enhanced three times in 3Q dimension as is seen from the difference in the mean frequencies of the doublets in 3Q dimension of the two enantiomers for **1** in Fig. 4. Values of these parameters scaled in the 3Q dimension are:
    (i) For (R/S)-2-chloropropionoic acid $3 \times \{T^S (=^3T_{H-H})\text{-}T^R (=^3T_{H-H})\} = 3 \times [17.3 - 16.4] = 3 \times [0.9] = 2.7$ Hz $\delta^R\text{-}\delta^S = 13.8$ Hz. in 3Q dimension

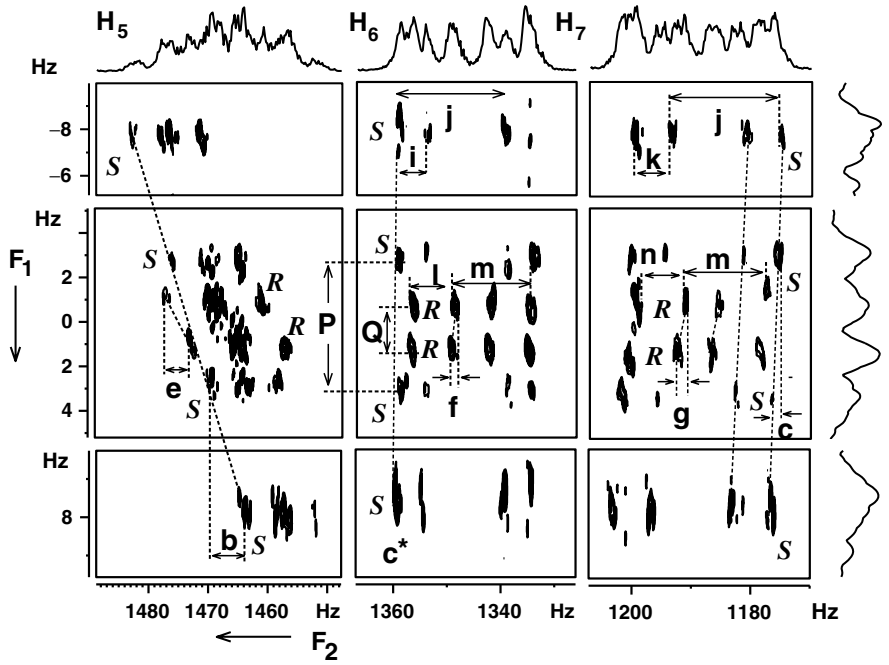

Fig. 10. Two dimensional 3Q–SQ correlation spectra of (*R*/*S*)-propylene oxide with selective excitation of protons numbered 5, 6 and 7. The 2D data matrix is 1331 × 48 zero filled to 2 k and 512 points before processing. The sine bell window function is used in both the dimensions. Eight scans for each FID and a recycle delay of 16 s. The optimized τ delay is 19.2 ms. The seduce shaped pulse lengths are 5 ms for both 90° and 180° pulses with different power levels. Digital resolution is 0.19 and 0.05 in F_1 and F_2 dimensions. For *S* enantiomer: $b = {}^3T_{H4H5} = 6.3$, $c = {}^4T_{H4H6} = -1.4$. c*($^4T_{H4H7}$ not detectable), $i = {}^3T_{H5H6} = 4.8$, $k = {}^3T_{H5H7} = 6.0$, $j = {}^3T_{H6H7} = 20$, For *R* enantiomer: $e = {}^3T_{H4H5} = 4.1$, $f = {}^4T_{H4H6} = -0.7$, $g = {}^4T_{H4H7} = -1.5$, $l = {}^3T_{H5H6} = 7.2$, $m = {}^3T_{H6H7} = 14.6$ and $n = {}^3T_{H5H7} = 8.6$.

(ii) For (*R*/*S*)-3-butyn-2-ol $3 \times \{T^R (={}^3T_{H-H})\text{-}T^S (={}^3T_{H-H})\} = 3 \times [48.9 - 32.4] = 3 \times [16.5] = 49.5$ Hz $3 \times \{T^R (={}^5T_{H-H})\text{-}T^S (={}^5T_{H-H})\} = 3 \times [8.95\text{-}8.8] = 3 \times [0.15] = 0.45$ Hz $\delta^R\text{-}\delta^S = 0.2$ Hz. in 3Q dimension.

From the above analysis it is observed that CSA enhanced discrimination is more dominating in the spectra of **1** while enhanced remote coupling assisted discrimination dominates in **2**. The advantage of CSA enhanced discrimination is lost in **3** and **4** due to the application of non-selective 180° pulse during the t_1 period.

(g) The displacement of the cross sections provides the relative signs of the passive couplings.

(h) In favourable cases, the parameters derived from the 2D spectra can be used for the iterative analysis to derive all other spectral parameters. This simplifies the analyses to a large extent.

As a result of the above discussed advantages, the peaks corresponding to *R* and *S* forms in SQ dimension appears in different cross sections which are well separated from each other. Thus the problem of overlap of the two spectra and hence doubling of transitions is also overcome. It can be pointed out that in the SERF experiment the chiral discrimination is achieved by removing the remote couplings and keeping short distance couplings in the indirect dimension. In such spectra the outer peaks get separated from each other because of the difference in short distance coupling for *R* and *S* enantiomers. However the central peaks are unresolved unlike in our experiment where even the central peaks of *R* and *S* enantiomers are separated as the two spectra never appear in the same cross section, exceptions being the case, when the peaks overlap due to comparable couplings. In SERF, DQ-SERF and BIRD inserted XH correlation experiments there is no spectral simplification in the direct dimension.

In general, the technique is applicable to any molecule. However, the requirement is the resonance of at least one group of protons should be isolated for selective excitation of higher quantum. In molecules with several interacting spins, the simultaneous excitation of several protons results in correspondingly higher quantum spectrum and consequently higher scaling factor and higher dispersion of the enantiomer peaks. As far as the limitation of the methodology is concerned, it is applicable to spin systems which provide first order spectra. If the spins are strongly coupled, the spin selective pulses cannot be applied and the question of determination of relative signs of the couplings do not arise.

5. Conclusions

The use of chiral liquid crystal for enantiomeric discrimination using proton as a passive spin by spin selective excitation of proton higher quantum coherence has been demonstrated. The inherent problem of lack of resolution and overlap in the proton spectrum has been overcome. The 3Q dimension of methyl protons excited 3Q–SQ exper-

iment containing fewer transitions provides three times scaling in the dipolar coupling between the selectively excited protons and the passive spin resulting in enhanced separation of the enantiomer peaks. Another significant advantage is the separation of the passive and active couplings which otherwise would provide broad and featureless one dimensional ^{1}H spectra. This important concept makes this methodology more superior to all the existing spectroscopic methods for chiral discrimination. Due to spin state selection, the cross sections along the direct dimension provided only the active couplings and hence higher resolution. The passive coupling information can be extracted from the projection of the displacement vector connecting peaks of like signs in the multiplet corresponding to the spin states of the passive nuclei. Chiral discrimination gets enhanced by three times scaling of the CSA in the 3Q dimension in favourable cases. The direction of tilt of the displacement vectors at difference chemical shift positions is an indicator of relative signs of the couplings. However, it is important to highlight the fact that SERF and DQ-SERF experiments do not provide relative signs of the couplings. The method utilizes every parameter determined from both SQ and 3Q dimensions for enantiomer visualization. With the combination of experiments, the complete analyses of broad and featureless ^{1}H spectra could be carried out and a measure of very small separation of the order of 0.7 Hz could be made. Thus ^{1}H detection for chiral discrimination which was hitherto considered as difficult or impossible has been demonstrated to be possible and the determination of ee may be routinely employed in future.

Acknowledgments

N.S. gratefully acknowledges the financial support by Department of Science and Technology, New Delhi for the Grant No. S(R/S)1/PC-13/2004. B.B. and U.R.P. thanks Council of Scientific and Industrial Research (CSIR) for research fellowship.

Appendix A. Supplementary data

Supplementary data associated with this article can be found, in the online version, at doi:10.1016/j.jmr.2008.02.005.

References

[1] D. Parker, NMR determination of enantiomeric purity, Chem. Rev. 91 (1991) 1441–1457.
[2] R. Rothchild, NMR methods for determination of enantiomeric excess, Enantiomer 5 (2000) 457–471.
[3] M. Sarfati, P. Lesot, D. Merlet, J. Courtieu, Theoretical and experimental aspects of enantiomeric differentiation using natural abundance multinuclear NMR spectroscopy in chiral polypeptide liquid crystals, Chem. Commun. (2000) 2069–2081.
[4] P. Lesot, D. Merlet, J. Courtieu, J.W. Emsley, T.T. Rantala, J. Jokisaari, Calculation of the molecular ordering parameters of (±)-3-butyn-2-ol dissolved in an organic solutions of poly-γ-benzyl-L-glutamate, J. Phys. Chem. A 101 (1997) 5719–5724.
[5] J. Farjon, D. Merlet, P. Lesot, J. Courtieu, Enantiomeric excess measurements in weakly oriented chiral liquid crystal solvents through 2D 1H selective refocusing experiments, J. Magn. Reson. 158 (2002) 169–172.
[6] L. Beguin, J. Courtieu, L. Ziani, D. Merlet, Simplification of the ^{1}H NMR spectra of enantiomers dissolved in chiral liquid crystals, combining variable angle sample spinning and selective refocusing experiments, Magn. Reson. Chem. 44 (2006) 1096–1101.
[7] A. Meddour, P. Berdague, A. Hedli, J. Courtieu, P. Lesot, Proton-decoupled carbon-13 NMR spectroscopy in a lyotropic chiral nematic solvent as an analytical tool for the measurement of the enantiomeric excess, J. Am. Chem. Soc. 119 (1997) 4502–4508.
[8] P. Lesot, D. Merlet, J. Courtieu, J.W. Emsley, Discrimination and analysis of the NMR Spectra of enantiomers dissolved in chiral liquid crystal solvents through 2D correlation experiments, Liquid Cryst. 21 (1996) 427–435.
[9] J. Farjon, J.P. Baltaze, P. Lesot, D. Merlet, J. Courtieu, Heteronuclear selective refocusing 2D NMR experiments for the spectral analysis of enantiomers in chiral oriented solvents, Magn. Reson. Chem. 42 (2004) 594–599.
[10] L. Ziani, J. Courtieu, D. Merlet, Visualisation of enantiomers via insertion of a BIRD module in X–H correlation experiments in chiral liquid crystal solvent, J. Magn. Reson. 183 (2006) 60–67.
[11] P. Lesot, O. Lafon, J. Courtieu, P. Berdagué, Analysis of the ^{13}C NMR spectra of molecules, chiral by isotopic substitution, dissolved in a chiral oriented environment: towards the absolute assignment of the pro-R/pro-S character of enantiotopic ligands in prochiral molecules, Chem. Eur. J. 10 (2004) 3741–3746.
[12] V. Madiot, P. Lesot, D. Grée, J. Courtieu, R. Gree, Highly enantioselective propargylic monofluorination established by carbon-13 and fluorine-19 NMR in chiral liquid crystals, Chem. Commun. (2000) 169–170.
[13] M. Jakubcova, A. Meddour, J.M. Péchiné, A. Baklouti, J. Courtieu, Measurement of the optical purity of fluorinated compounds using proton decoupled ^{19}F NMR spectroscopy in a chiral liquid crystal solvent, J. Fluorine Chem. 86 (1997) 149–153.
[14] I. Canet, J. Courtieu, A. Loewenstein, A. Meddour, J.M. Péchiné, Enantiomeric analysis in polypeptide lyotropic liquid crystal by deuterium NMR, J. Am. Chem. Soc. 117 (1995) 6520–6526.
[15] D. Merlet, B. Ancian, J. Courtieu, P. Lesot, Two-dimensional deuterium NMR spectroscopy of chiral molecules oriented in a polypeptide liquid crystal: application for the enantiomeric analysis through natural abundance deuterium NMR, J. Am. Chem. Soc. 121 (1999) 5249–5258.
[16] D. Merlet, M. Sarfati, B. Ancian, J. Courtieu, P. Lesot, Description of natural abundance deuterium 2D-NMR experiments in weakly ordered liquid-crystalline solvents using a tailored Cartesian spin-operator formalism, Phys. Chem. Chem. Phys. 2 (2000) 2283–2290.
[17] P. Lesot, D. Merlet, A. Loewenstein, J. Courtieu, Enantiomeric visualisation using proton-decoupled natural abundance deuterium NMR in PBLG liquid crystalline solutions, Tetrahedron: Asymmetry 9 (1998) 1871–1881.
[18] D. Merlet, B. Ancian, W. Smadja, J. Courtieu, P. Lesot, Analysis of natural abundance deuterium NMR spectra of enantiomers in chiral liquid crystals via 2D auto-correlation experiments, Chem. Commun. (1998) 2301–2302.
[19] A. Meddour, C. Canlet, L. Blanco, J. Courtieu, Diastereomeric shape recognition using NMR spectroscopy in a chiral liquid crystalline solvent, Angew. Chem. Int. Ed. 38 (1999) 2391–2393.
[20] J. Jarvet, P. Allard, Phase-sensitive two-dimensional heteronuclear zero- and double-quantum-coherence spectroscopy, J. Magn. Reson. B 112 (1996) 240–244.
[21] P. Permi, S. Heikkinen, I. Kilpeläinen, A. Annila, Measurement of homonuclear ^{2}J-couplings from spin-sate selective double-/zero-quantum two-dimensional NMR spectra, J. Magn. Reson. 139 (1999) 273–280.

[22] G. Otting, A DQ/ZQ NMR experiment for the determination of the signs of small J(^{1}H,^{13}C) coupling constants in linear spin systems, J. Magn. Reson. 124 (1997) 503–505.
[23] A. Rexroth, P. Schmidt, S. Szalma, T. Geppert, H. Schwalbe, C. Griesinger, New principle for the determination of coupling constants that largely suppresses differential relaxation effects, J. Am. Chem. Soc. 117 (1995) 10389–10390.
[24] P. Andersson, J. Weigelt, G. Otting, Spin-state selection filters for the measurement of heteronuclear one-bond coupling constants, J. Biomol. NMR 12 (1988) 435–441.
[25] B. Brutscher, Accurate measurement of small spin–spin couplings in partially aligned molecules using a novel J-mismatch compensated spin-state-selection filter, J. Magn. Reson. 151 (2001) 332–338.
[26] P. Permi, Determination of three-bond scalar couplings between $^{13}C'$ and $^1H^{\alpha}$ in protein using an iHN(CA),CO(α/β-J-COHA) experiment, J. Magn. Reson. 163 (2003) 114–120.
[27] L. Duma, S. Hediger, A. Lesage, L. Emsley, Spin-state selection in solid-state NMR, J. Magn. Reson. 164 (2003) 187–195.
[28] L. Duma, S. Hediger, B. Brutscher, A. Böckmann, L. Emsley, Resolution enhancement in multidimensional solid-state NMR spectroscopy of proteins using spin-state selection, J. Am. Chem. Soc. 125 (2003) 11816–11817.
[29] P. Nolis, J.F. Espinosa, T. Parella, Optimum spin-state selection for all multiplicities in the acquisition dimension of the HSQC experiment, J. Magn. Reson. 180 (2006) 39–50.
[30] R. Verel, T. Manolikas, A.B. Siemer, B.H. Meier, Improved resolution in ^{13}C solid-state spectra through spin-state-selection, J. Magn. Reson. 184 (2007) 322–329.
[31] P. Permi, A. Annila, A new approach for obtaining sequential assignment of large proteins, J. Biomol. NMR 20 (2001) 127–133.
[32] P. Permi, A. Annila, Transverse relaxation optimized spin-state selective NMR experiments for measurement of residual dipolar couplings, J. Biomol. NMR 16 (2000) 221–227.
[33] P. Permi, A spin-state-selective experiment for measuring heteronuclear one-bond and homonuclear two-bond couplings from an HSQC-type spectrum, J. Biomol. NMR 22 (2002) 27–35.
[34] D. Lee, B. Vögeli, K. Pervushin, Detection of C', C_α correlations in proteins using a new time- and sensitivity optimal-experiment, J. Biomol. NMR 31 (2005) 273–278.
[35] P. Würtz, K. Fredriksson, P. Permi, A set of HA-detected experiments for measuring scalar and residual dipolar couplings, J. Biomol. NMR 31 (2005) 321–330.
[36] C.R.R. Grace, R. Riek, Pseudomultidimensional NMR by spin-state selective off-resonance decoupling, J. Am. Chem. Soc. 125 (2003) 16104–16113.
[37] P. Nolis, T. Parella, Simultaneous spin-state α/β selection for ^{13}C and ^{15}N from a time-shared HSQC-IPAP experiment, J. Biomol. NMR 37 (2007) 65–77.
[38] P.R. Vasos, J.B. Hall, D. Fushmann, Spin-state selection for increased confidence in cross-correlation rates measurements, J. Biomol. NMR 31 (2005) 149–154.
[39] B. Baishya, N. Suryaprakash, Spin state selective detection of single quantum transitions using multiple quantum coherence: simplifying the analyses of complex NMR spectra, J. Phys. Chem. A 111 (2007) 5211–5217.
[40] B. Baishya, U.R. Prabhu, N. Suryaprakash, Enantiomeric discrimination by double quantum excited selective refocusing (DQ-SERF) experiment, J. Phys. Chem. B 111 (2007) 12403–12410.
[41] A. Bax, R. Freeman, T.A. Frenkiel, M.H. Levitt, Assignment of carbon-13 NMR spectra via double-quantum coherence, J. Magn. Reson. 43 (1981) 478–483.
[42] O.W. Sørensen, G.W. Eich, M.H. Levitt, G. Bodenhausen, R.R. Ernst, Product operator formalism for the description of NMR pulse experiments, Prog. NMR Spectrosc. 16 (1983) 163–192.
[43] T.J. Norwood, Multiple quantum NMR methods, Prog. NMR Spectrosc. 24 (1992) 295–375.
[44] B. Baishya, N. Suryaprakash, Spin selective multiple quantum NMR for spectral simplification, determination of relative signs and magnitudes of scalar couplings by spin state selection, J. Chem. Phys. 127 (2007) 214510.